ISSN 1001-0742
CN 11-2629/X

JES

JOURNAL OF ENVIRONMENTAL SCIENCES

April 1, 2015 Volume 30
www.jesc.ac.cn

MBR in Wastewater Reclamation

ELSEVIER
Science Press

Sponsored by
Research Center for Eco-Environmental Sciences
Chinese Academy of Sciences

Journal of Environmental Sciences Volume 30 2015

www.jesc.ac.cn

Highlight articles

Review articles

Regular articles

CONTENTS

Available online at www.sciencedirect.com

ScienceDirect

www.journals.elsevier.com/journal-of-environmental-sciences

JOURNAL OF ENVIRONMENTAL SCIENCES
www.jesc.ac.cn

Removal kinetics of phosphorus from synthetic wastewater using basic oxygen furnace slag

Chong Han, Zhen Wang, He Yang, Xiangxin Xue*

School of Materials & Metallurgy, Northeastern University, Shenyang 110819, China. E-mail: hanch@smm.neu.edu.cn

ARTICLE INFO

Article history:
Received 1 May 2014
Revised 4 November 2014
Accepted 13 November 2014
Available online 20 February 2015

Keywords:
Basic oxygen furnace slag
Phosphorus
Kinetics
Apparent rate constant

ABSTRACT

Removal kinetics of phosphorus through use of basic oxygen furnace slag (BOF-slag) was investigated through batch experiments. Effects of several parameters such as initial phosphorus concentration, temperature, BOF-slag size, initial pH, and BOF-slag dosage on phosphorus removal kinetics were measured in detail. It was demonstrated that the removal process of phosphorus through BOF-slag followed pseudo-first-order reaction kinetics. The apparent rate constant (k_{obs}) significantly decreased with increasing initial phosphorus concentration, BOF-slag size, and initial pH, whereas it exhibited an opposite trend with increasing reaction temperature and BOF-slag dosage. A linear dependence of k_{obs} on total removed phosphorus (TRP) was established with $k_{obs} = (3.51 \pm 0.11) \times 10^{-4} \times TRP$. Finally, it was suggested that the Langmuir–Rideal (L–R) or Langmuir–Hinshelwood (L–H) mechanism may be used to describe the removal process of phosphorus using BOF-slag.

Introduction

Phosphorus is an essential nutrient for the growth of plants and animals. However, the enrichment of phosphorus in water bodies including rivers, lakes, and lagoons can give rise to abnormal growth of hydrophytes, which results in the deterioration of water quality and finally leads to eutrophication. Thus, phosphorus should be removed from domestic and industrial wastewater before being discharged into the surrounding environment. Constructed wetland systems (CWS) have been demonstrated as an effective treatment method for phosphorus removal (Barca et al., 2013; Johansson-Westholm, 2006; Shilton et al., 2006; Vohla et al., 2011). The selection of the materials for wetland substrates plays a key role in designing the CWS (Drizo et al., 2006). Many low cost and easily available materials such as natural minerals (limestone (Johansson-Westholm, 2006), zeolites (Johansson-Westholm, 2006), bauxite (Johansson-Westholm, 2006), and dolomite (Karaca et al., 2006)) and industrial by-products such as fly ash (Cheung and Venkitachalam, 2000; Li et al., 2006), dewatered alum sludge (Yang et al., 2006), coal cinders (Wang et al., 2010), iron oxide tailings (Zeng et al., 2004), and blast furnace slag (Gong et al., 2009; Oguz, 2005; Kostura et al., 2005) have been assessed for their capacity to sequester phosphorus.

In the last decades, the by-products (basic oxygen furnace slag and electric arc furnace slag) from the steel industry have attracted considerable interest from researchers to investigate them as appropriate wetland substrates through various methods such as batch tests (Bowden et al., 2009; Barca et al., 2012; Jha et al., 2004, 2008; Xiong et al., 2008; Xue et al., 2009), column tests (Cha et al., 2006; Claveau-Mallet et al., 2012, 2013; Yang et al., 2009) and field tests (Barca et al., 2013; Lee et al., 2010; Shilton et al., 2006). Basic oxygen furnace slag (BOF-slag) is derived from the refining of iron in a basic oxygen furnace, whereas electric arc furnace slag (EAF-slag) originates from melting recycled scrap in an electric arc furnace (Barca et al.,

* *Corresponding author.*

http://dx.doi.org/10.1016/j.jes.2014.11.003

2013). Steel slag consists of heterogeneous oxide materials and is primarily composed of species containing iron, calcium, aluminum and silicon (Xue et al., 2009).

According to the results of different studies, the removal rate of phosphorus by steel slag greatly varied in the range of 37%–100% and its phosphorus removal capacity drastically fluctuated from 0.13 to 89.9 mg P/g (Barca et al., 2012, 2013; Bowden et al., 2009; Claveau-Mallet et al., 2013; Drizo et al., 2006; Li et al., 2013; Wang et al., 2010; Xiong et al., 2008; Yang et al., 2009). These large discrepancies significantly depended on various factors such as exposure duration of phosphorus to steel slag, temperature, phosphorus concentration, wastewater pH, steel slag dosage, steel slag size, and chemical composition of steel slag. There have been two popular mechanisms for phosphorus removal by steel slag. A number of researchers have concluded that the main mechanism of phosphorus removal was related to CaO-slag dissolution followed by Ca–P precipitation (Barca et al., 2012, 2013; Bowden et al., 2009; Claveau-Mallet et al., 2012, 2013; Drizo et al., 2006). Nevertheless, other studies have suggested the adsorption of phosphorus onto metal oxides/oxyhydroxides on the surface of steel slag to be a primary phosphorus removal mechanism (Jha et al., 2008; Pratt et al., 2007a,b; Xiong et al., 2008; Xue et al., 2009).

To date, researchers have focused on the investigation of phosphorus removal capacity of steel slag as well as the mechanism. However, few studies have been performed to determine the kinetics of phosphorus removal by steel slag. Jha et al. (2008) suggested that a first order rate expression was more appropriate than the pseudo-second order equation for the data obtained from batch experiments. The phosphorus removal data of CWS with steel slag as filter substrates can be also well explained employing the model of Kadlec and Knight, which originated from the first-order kinetics equation proposed by the U.S. Environmental Protection Agency to model pollutant removal in CWS (Barca et al., 2013). It should be pointed out that the understanding of phosphorus removal kinetics using steel slag is still limited. The study of phosphorus removal kinetics can substantially contribute to the understanding of the whole process and the mechanism of phosphorus removal by steel slag.

In this work, therefore, the kinetics of phosphorus removal by BOF-slag was analyzed in detail through batch experiments. Fresh and reacted BOF-slag was characterized using an X-ray diffractometer (XRD) and scanning electron microscope (SEM) equipped with an energy dispersive spectrometer (EDS) system. Effects of several parameters, including initial phosphorous concentration, temperature, steel slag size, initial pH, and steel slag dosage, on the reaction rate of phosphorus removal were investigated. A quantitative relationship between reaction rate of phosphorus removal and total removed phosphorus was also established. Finally, Langmuir–Hinshelwood (L–H) and Langmuir–Rideal (L–R) mechanisms were discussed and used to describe the phosphorus removal process, which may help reveal the mechanism of phosphorus removal by steel slag.

1. Experimental

1.1. Materials

BOF-slag was from Anshan Iron and Steel Group Corporation in Liaoning province of China. The chemical composition of BOF-slag was analyzed using X-ray fluorescence (XRF). The composition of BOF-slag was mainly CaO (47.08%), Fe_2O_3 (36.12%), SiO_2 (8.04%), and MgO (4.94%), with small amount of MnO (1.99%), Al_2O_3 (0.78%), TiO_2 (0.56%), P_2O_5 (0.30%), Cr_2O_3 (0.15%), SrO (0.03%), and Nb_2O_5 (0.02%). This is similar to steel slag used in previous studies (Barca et al., 2013; Bowden et al., 2009; Claveau-Mallet et al., 2012). To obtain samples with different sizes (0–0.038, 0.038–0.045, 0.045–0.058, 0.058–0.106, 0.106–0.180 mm), BOF-slag was ground into fine powders and sieved through sieves of different mesh sizes.

1.2. Batch experiments

A series of batch tests was conducted to investigate the influence of several parameters on the kinetics of phosphorus removal by BOF-slag. Synthetic wastewater with different initial phosphorus concentrations (50, 75, 100 and 125 mg P/L) was prepared using tap water and KH_2PO_4 as the phosphorus source. Then, BOF-slag with different sizes was added to beakers containing 250 mL synthetic wastewater. The BOF-slag dosage varied in the range 0.0–2.0 g. The solution in the beaker was continuously stirred for 4.0 hr employing a stirring apparatus with a temperature control system. The reaction temperature could be exactly controlled from 293 to 313 K. The initial solution pH was adjusted to desired values using 0.05 mol/L HCl and 0.05 mol/L NaOH. The pH was measured using a pH meter (PHS-3C Model, Shanghai Precision & Scientific Instrument Co.Ltd, Shanghai, China). The solution was sampled at certain time intervals and centrifuged at 3000 r/min for 5.0 min to separate BOF-slag from the liquid phase.

1.3. Kinetics analysis

The Langmuir–Rideal (L–R) mechanism is usually used to describe heterogeneous reaction processes. This mechanism indicates the reaction between liquid phase phosphorus ($[P_{liq}]$) and active species ([AS]) on the surface of BOF-slag as shown in Eq. (1).

$$[AS] + [P_{liq}] \rightarrow \text{Products} \quad (1)$$

The kinetics of Eq. (1) can be described using Eq. (2).

$$\frac{d[P_{liq}]}{dt} = -k^{II} \times [AS] \times [P_{liq}] \quad (2)$$

where, k^{II} is the second order rate constant. A pseudo first-order kinetics can be assumed by replacing $k^{II} \times [AS]$ with k_{obs}, which is the apparent rate constant.

$$\frac{d[P_{liq}]}{[P_{liq}]} = -k_{obs} \times dt \quad (3)$$

Eq. (4) derives from the integration of Eq. (3).

$$\frac{1}{t} \ln\left(\frac{[P_{liq}]_0}{[P_{liq}]_t}\right) = k_{obs} = k^{II} \times [AS] \quad (4)$$

Thus, k^{II} can be obtained through linear fitting of k_{obs} as a function of [AS].

Additionally, the Langmuir–Hinshelwood (L–H) mechanism may also occur during the phosphorus removal process using BOF-slag. According to this mechanism, the reaction can occur when active species on the surface of BOF-slag encounter phosphorus adsorbed on adjacent sites. The k_{obs} can be expressed by the following equation in the L–H mechanism,

$$\frac{k^{II}[SS]K_{AS}[AS]}{1 + K_{AS}[AS]} = k_{obs} \quad (5)$$

where, k^{II} is the second order rate coefficient, [SS] is the number of adsorption sites for active species of BOF-slag, K_{AS} is the liquid-surface equilibrium constant of active species of BOF-slag, and [AS] is the total number of active species. k^{II}[SS] can be approximated as the maximum rate coefficient k^{I}_{max} experimentally obtained at high BOF-slag dosage. Therefore, Eq. (6) can be obtained through replacing k^{II}[SS] with k^{I}_{max} in Eq. (5).

$$\frac{k^{I}_{max}K_{AS}[AS]}{1+K_{AS}[AS]} = k_{obs} \quad (6)$$

The parameters k^{I}_{max} and K_{AS} can be obtained through fitting k_{obs} as a function of [AS] using Eq. (6). It should be pointed out that [AS] can be replaced with BOF-slag dosage due to their positive relationship.

1.4. Analysis methods

The change of phosphorus concentration with reaction time was measured according to the ammonium molybdate spectrometric method using a UV–Visible spectrophotometer (UV–vis, UV-2550, SHIMADZU, Kyoto Japan). The change in Ca^{2+} concentration when BOF-slag was introduced into tap water was detected by the atomic absorption spectrometric method (AAS, TAS-990, Beijing Purkinje General Instrument Co. Ltd, Beijing, China). Batch test data were modeled to analyze the phosphorus removal kinetics. The mineral compositions of fresh and reacted BOF-slag were investigated through XRD (X' Pert Pro, PANalytical, Almelo, Netherlands) with Cu $K\alpha$ radiation at 40 kV and 300 mA. The scanned range was 2θ = 10°–90° with a step of 2θ = 0.05° and 1 sec/step. SEM-EDS (SSX-550, SHIMADZU, Kyoto, Japan) were used to investigate the morphology and elemental composition of fresh and reacted BOF-slag. The specific surface area of BOF-slag with different sizes was measured by a laser particle size analyzer (BT-9300S, Dandong Bettersize Instruments Ltd., Dandong, China).

2. Results

2.1. Changes of composition and morphology of BOF-slag

Fig. 1 shows XRD patterns of fresh and reacted slag. According to the XRD results, fresh BOF-slag primarily consisted of calcium- and iron-bearing mineral phases including srebrodolskite, calcium silicate, merwinite, fayalite, bredigite, lime, wustite, and so on. The presence of these minerals indicates that the fresh BOF-slag has the potential to remove phosphorus from wastewater through adsorption or precipitation. Compared to the pattern of fresh BOF-slag, intensities of some peaks of the reacted BOF-slag decreased, which can be ascribed to the hydrolysis of $Ca_2Fe_2O_5$, Ca_2SiO_4, $Ca_{14}Mg_2(SiO_4)_8$, $Ca_3Mg(SiO_4)_2$, $CaFe_2O_4$, CaO, and FeO. After the introduction of BOF-slag (1.0 g) into tap water (250 mL) without phosphate, the Ca^{2+} concentration in tap water increased by 18.2 mg/L, further proving the hydrolysis of species containing calcium in BOF-slag. It has been previously shown that $Ca_{14}Mg_2(SiO_4)_8$ was the first calcium oxide that dissolved during the phosphorus removal process

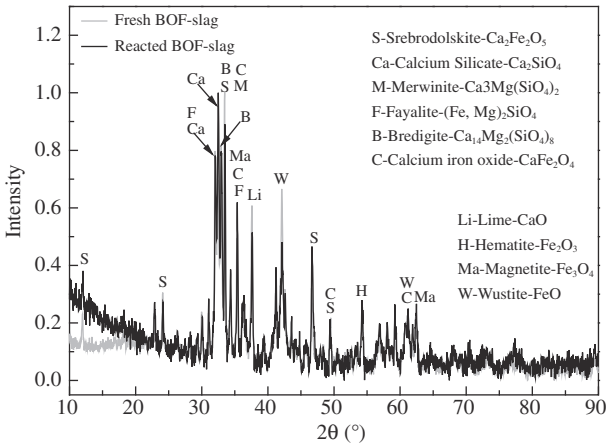

Fig. 1 – X-ray diffractometer (XRD) pattern of fresh and reacted BOF-slag under conditions with BOF-slag (0.038–0.045 mm) of 1.0 g, initial phosphorus concentration of 100 mg/L, initial pH of 7.0, and temperature of 298 K.

using furnace slag (Kostura et al., 2005). Barca et al. (2012) confirmed that Ca^{2+} and OH^- from BOF-slag hydrolysis followed a pseudo-first-order kinetics model. Notably, no peaks related to Ca-phosphate precipitates were found in the XRD pattern, which may be attributed to several reasons. On the one hand, the mass of Ca-phosphate precipitates may be lower than the detection limit of XRD. On the other hand, the Ca-phosphate precipitates may be amorphous. Of course, there also may not be any formation of Ca-phosphate precipitates.

The surface of fresh and reacted BOF-slag was examined by SEM and EDS analyses. The morphology of fresh and reacted BOF-slag exhibited differences, as shown in Fig. 2a and c. The surface of the reacted BOF-slag seemed to be covered with finely distributed layers. According to Fig. 2b, the EDS results confirmed that the surface of fresh BOF-slag was mainly composed of O, Ca and Fe. However, as shown in Fig. 2d, the fine layers on the reacted BOF-slag predominantly consisted of O, Ca, Fe, Si, and P. This suggests that the fine layers may be related to the interaction of phosphorus with species on BOF-slag.

2.2. Phosphorus removal kinetics

Fig. 3a shows temporal changes of phosphorus with different initial concentrations. Phosphorus concentration exhibited a significant decrease upon the addition of BOF-slag. It was observed that phosphorus with initial concentration of 50 mg/L had been completely removed at the reaction time of 60 min, demonstrating that BOF-slag is an efficient substrate, as proposed by previous studies (Barca et al., 2012, 2013; Claveau-Mallet et al., 2012, 2013). The temporal removal trend of phosphorus greatly decreased with increasing initial concentration from 50 to 125 mg/L. In particular, the evolution of phosphorus with different initial concentrations showed an exponential pattern, suggesting that the removal reaction of phosphorus by BOF-slag may be reasonably described by pseudo-first-order kinetics. Therefore, the batch experimental data may be fitted using a pseudo-first-order exponential

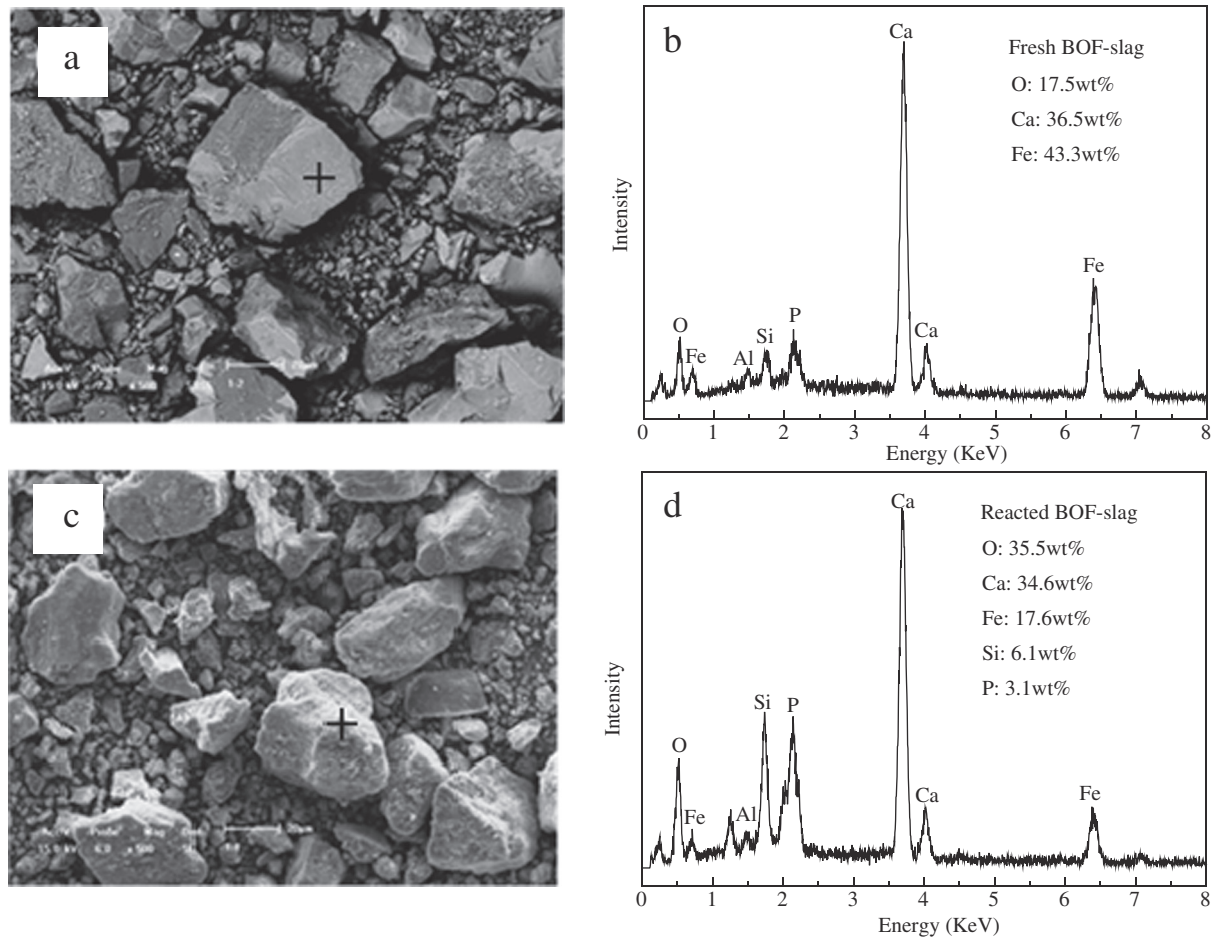

Fig. 2 – SEM observations of fresh (a) and reacted (c) BOF-slag, respectively; EDS results of fresh (b) and reacted (d) BOF-slag, respectively. The area generating the EDS spectra has been pointed by " + " in the SEM images. Reaction conditions are BOF-slag (0.038–0.045 mm) of 1.0 g, initial phosphorus concentration of 100 mg/L, initial pH of 7.0, and temperature of 298 K.

function as shown in Eq. (3) or (4). Fig. 3b displays the linear correlation between the natural logarithm of phosphorus concentration and reaction time. Jha et al. (2008) also found that the first-order equation was appropriate to describe the removal process of phosphorus by mixtures of steel-making slag with $Al(OH)_3$. Additionally, the data of phosphorus removal through simulated CWS can be also well analyzed using the model derived from the first-order kinetics equation (Barca et al., 2013). Therefore, these results demonstrate the pseudo-first-order reaction nature of phosphorus with BOF-slag.

As shown in Fig. 4a, k_{obs} exhibited a noticeable decrease trend with increasing initial phosphorus concentration. k_{obs} was 5.79×10^{-2} min^{-1} at initial phosphorus concentration of 50 mg/L, whereas it was only 0.39×10^{-2} min^{-1}, lower by 93.3%, at initial phosphorus concentration of 125 mg/L. k_{obs} drastically decreased from 5.79×10^{-2} to 1.25×10^{-2} min^{-1} with increasing initial phosphorus concentration from 50 to 75 mg/L, with only slight further decrease when the initial phosphorus concentration was more than 75 mg/L.

Temperature can affect the removal efficiency of phosphorus, as already shown in field experiments with steel slag as filter medium (Barca et al., 2013; Shilton et al., 2006). It has been observed in practice that the efficiency decreased drastically during winter and then began to gradually increase during spring (Barca et al., 2013; Shilton et al., 2006). However, little is known about effects of temperature on phosphorus removal kinetics. Fig. 4b shows an increase trend for k_{obs} with increasing temperature. k_{obs} at temperature of 313 K was larger by 47.6% than that at temperature of 293 K. Although k_{obs} almost remained unchanged in the range of 293–303 K, it exhibited a significant increase with increasing temperature from 303 to 313 K.

The change trend of k_{obs} with increasing BOF-slag size was investigated as shown in Fig. 4c. k_{obs} significantly decreased with increasing BOF-slag size in the range of 0.00–0.180 mm. k_{obs} was 3.8×10^{-3} min^{-1} and lower by 28.0% at BOF-slag size of 0.106–0.180 mm than that at BOF-slag size of 0.00–0.038 mm.

Fig. 4d shows that k_{obs} greatly decreased with increasing initial pH from 3.0 to 7.0. k_{obs} was 8.3×10^{-3} min^{-1} at initial pH of 3.0 but it was 4.8×10^{-3} min^{-1} and lower by 42.2% at initial pH of 7.0. As seen in Fig. 4e, although great differences existed in initial pH, the final pH remained stable around pH of 7.5–7.8 after reaction for 4.0 hr. Yang et al. (2009) also observed a similar phenomenon during the phosphorus removal progress using converter slag and coal cinders. The increase of pH

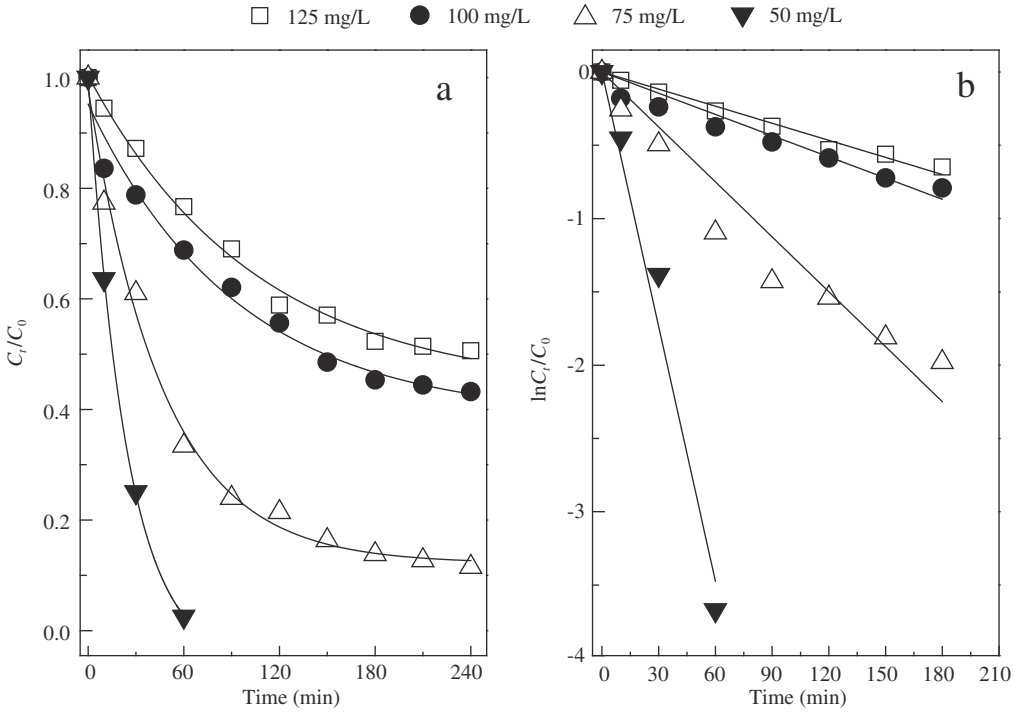

Fig. 3 – Temporal changes of phosphorus with different initial concentrations (a) and kinetics fitting results of phosphorus (b) under conditions with BOF-slag (0.038–0.045 mm) of 1.0 g, initial pH of 7.0, and temperature of 298 K.

can be ascribed to the hydrolysis of components containing metals (Barca et al., 2012; Xue et al., 2009), which has been illustrated in Fig. 1. It should be pointed out that Ca^{2+} and Mg^{2+} in tap water under alkaline conditions can react with OH^- or PO_4^{3-} to form a white precipitate without the addition of BOF-slag. This may influence the measurement of phosphorus and lead to the impracticability conducting experiments at pH higher than 8.0.

As seen in Fig. 4f, k_{obs} exhibited a great increase with increasing BOF-slag dosage. However, k_{obs} did not linearly depend on BOF-slag dosage. k_{obs} at BOF-slag dosage of 2.0 g increased by 53.3% when compared to that at BOF-slag dosage of 0.5 g.

The results mentioned above definitely demonstrate that the parameters including initial phosphorus concentration, temperature, BOF-slag size, initial pH, and BOF-slag dosage have important influences on the kinetics of phosphorus removal by BOF-slag.

2.3. Relationship between k_{obs} and total removed phosphorus

It has been widely demonstrated that several parameters including slag size, initial pH, and slag dosage, have significant effects on the phosphorus removal capacity (Bowden et al., 2009; Xiong et al., 2008; Xue et al., 2009; Yang et al., 2009). As seen from Fig. 4b, total removed phosphorus (TRP) tended to increase with increasing temperature. As shown in Fig. 4c and d, TRP decreased with increasing BOF-slag size and increasing initial pH from acidity to neutral, respectively. TRP gradually increased with increasing BOF-slag dosage, while the removed phosphorus per unit mass exhibited an opposite trend (Fig. 4f). This indicates that some of the BOF-slag cannot reach its potential to sequester phosphorus at higher dosage. Phosphorus removal capacity varied in the range of 11.4–20.3 mg/g under the varying conditions in this work. However, maximum phosphorus removal capacity has been reported to range from 0.13 to 89.9 mg/g. This great difference can be ascribed to the variation of main parameters such as contact time of phosphorus with slag, temperature, initial phosphorus concentration, pH, ratio of slag to solution, particle size, and structure and composition of slag, which can affect the results of batch experiments (Barca et al., 2012).

Based on careful comparison, it was found that the change trend of k_{obs} was similar to that of TRP under the corresponding reaction conditions. This suggests that there may be a certain relationship between k_{obs} and TRP. As shown in Fig. 5, k_{obs} linearly increased with increasing TRP, and the slope was $(3.51 \pm 0.11) \times 10^{-4}$ $min^{-1} \cdot mg^{-1}$. Thus, a quantitative dependent relationship between k_{obs} and TRP can be simply established and expressed as $k_{obs} = (3.51 \pm 0.11) \times 10^{-4} \times TRP$. Therefore, TRP can be roughly estimated as long as k_{obs} has been measured. This will provide convenience in obtaining the phosphorus removal capacity (PRC) of BOF-slag, since long-term tests are usually required to obtain the PRC of steel slag.

2.4. Applicability of L–R and L–H mechanism for phosphorus removal kinetics

Fig. 6 shows the fitted results of k_{obs} as a function of BOF-slag dosage according to the L–R and L–H mechanisms, R^2 of which was 0.965 and 0.964, respectively. According to the fitted results,

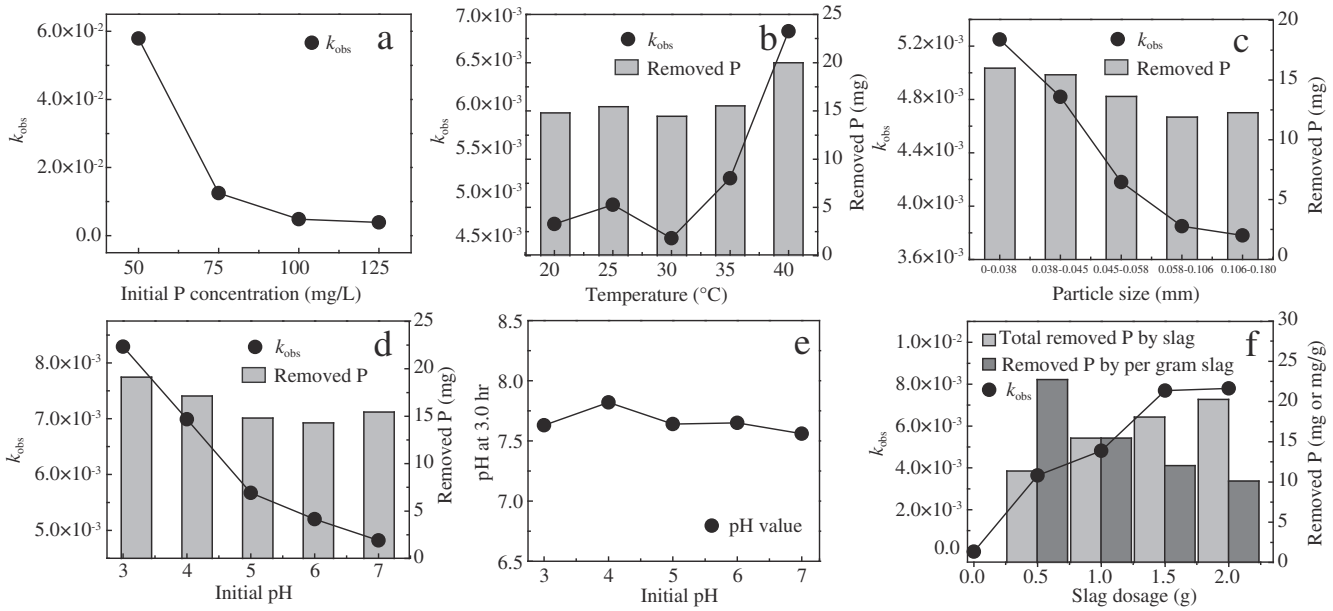

Fig. 4 – Changes of k_{obs} under various conditions (a, b, c, d, and f) and changes of pH after the reaction for 4.0 hr (e). Reaction conditions were summarized in Table S1.

k^{II}, k^{I}_{max}, and K_{AS} were (4.5 ± 0.38) × 10^{-3}, (1.49 ± 0.38) × 10^{-2}, and (0.58 ± 0.31) $min^{-1}·g^{-1}$, respectively. In view of the fitted results, both the L–R and L–H mechanisms can well describe the kinetics of phosphorus removal by BOF-slag. This leads to difficulty in picking out one or the other mechanism.

It has been demonstrated that pH has extremely important effects on mechanisms of phosphorus removal by steel slag. The adsorption of phosphorus to metal oxide surfaces plays a critical role at pH lower than 7.5, while Ca-phosphate precipitation is the dominant removal mechanism at pH higher than 8.0 (Bowden et al., 2009; Khelifi et al., 2002; Søvik and Kløve, 2005). According to the pH (7.5–7.8) after the reaction for 4.0 hr (Fig. 4e), the adsorption to metal oxide surfaces in BOF-slag should account for most of phosphorus removal for solutions with initial pH of 3.0–7.0.

XRF and XRD results have determined that BOF-slag is rich in Fe and Ca oxide. It is well known that Fe and Ca play important roles in phosphorus removal by steel slag. The mechanism of Fe for phosphorus removal has been suggested to be an adsorption process onto Fe oxides/hydroxides (Pratt et al., 2007a). The adsorption process of phosphorus can also occur through ligand exchange between phosphate and hydroxide groups on the surface of silicon and aluminum oxides in steel slag (Xue et al., 2009). The existence of P together with Fe and Si in fine layers on the reacted BOF-slag suggests the occurrence of these adsorption processes (Fig. 2b, d). As mentioned above, these adsorption processes were main removal paths for phosphorus, which supports the application of the L–R or L–H mechanism to phosphorus removal by BOF-slag. Additionally, the hydrolysis of components containing calcium such as CaO, $Ca_{14}Mg_2(SiO_4)_8$, $Ca_2Al_2SiO_7$, Ca_2SiO_4, and Ca_3SiO_5 can lead to the release of Ca and the increase of pH (Cha et al., 2006; Claveau-Mallet et al., 2012, 2013; Kostura et al., 2005). Under basic conditions, the mechanism of Ca in phosphorus retention was the formation of various Ca-phosphate precipitates including amorphous calcium phosphate (ACPs), dicalcium phosphate (DCP), dicalcium phosphate dihydrate (DCPD), octocalcium phosphate (OCP), tricalcium phosphate (TCP), and hydroxyapatite (HAP) (House, 1999; Valsami-Jones, 2001). Previous studies generally suggested that these Ca-phosphate precipitates were derived from the liquid phase reaction of calcium with phosphate (Barca et al., 2012, 2013; Claveau-Mallet et al., 2013). In fact, the dissolution of Ca may be incomplete or reach an equilibrium between the liquid phase and the BOF-slag surface. Moreover, the solubility of Ca-phosphate precipitates is far less than the components containing calcium. Thus, the adsorbed phosphate may capture the undissolved Ca on adjacent surface sites, resulting in the formation of Ca-phosphate precipitates. This may also take part in the reaction of the adsorbed phosphorus and active species on BOF-slag in L–H mechanism. Further studies may be necessary to better determine the applicability of the L–R or L–H mechanism for the phosphorus removal process.

3. Discussion

It is time to step back and discuss the effects of several parameters on phosphorus removal kinetics. As shown in Fig. S1, the natural logarithm of k_{obs} linearly decreased with increasing reciprocal temperature in the range of 303–313 K. According to the Arrhenius equation, an apparent activation energy (E_a) and pre-exponential factor (A) can be calculated, and were (3.35 ± 0.67) × 10^4 J/mol and (2.44 ± 0.01) × 10^3 min^{-1}, respectively. Positive E_a further suggests that the increase of temperature can accelerate phosphorus removal by BOF-slag.

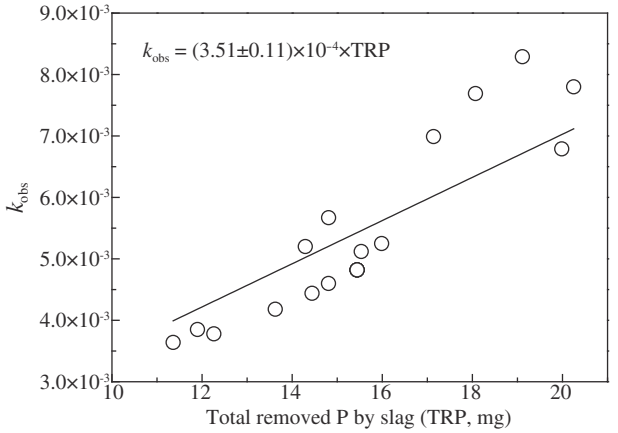

Fig. 5 – Plot of k_{obs} versus total removed phosphorus (TRP) by slag.

The distribution coefficient (K_D, cm^3/g) of phosphorus on BOF-slag and in solution can be described by the following equation (Oguz, 2005),

$$K_D = \frac{V}{M} \quad (7)$$

where, V is the solution volume of phosphorus on BOF-slag and M is the phosphorus mass of BOF-slag. Standard enthalpy ($\triangle H^0$) and standard entropy ($\triangle S^0$) can be calculated from the slope and intercept of linear regression of $\ln(K_D)$ against $1/T$ (Eq. (8)),

$$\ln(K_D) = \frac{\Delta S^0}{R} - \frac{\Delta H^0}{RT} \quad (8)$$

where, T (K) is the absolute temperature and R (J/(mol·K)) is the gas constant. The standard free energy ($\triangle G^0$) can be obtained from Eq. (9).

$$\Delta G^0 = \Delta H^0 - T\Delta S^0 \quad (9)$$

As seen in Fig. S2, K_D exhibited a linearly increasing relationship with the increase of temperature. $\triangle H^0$ and $\triangle S^0$ were calculated to be (5.70 ± 2.39) × 10^4 J/mol and (2.34 ± 0.77) × 10^2 J/(mol · K), respectively. Positive $\triangle H^0$ confirmed that the adsorption of phosphorus on BOF-slag was an endothermic process. According to Eq. (9), $\triangle G^0$ would decrease with the increase of temperature. These results suggest that the adsorption of phosphorus on BOF-slag is easier at higher temperature. Thus, changes of k_{obs} with increasing temperature may be related to the effects of temperature on the adsorption process of phosphorus to active sites.

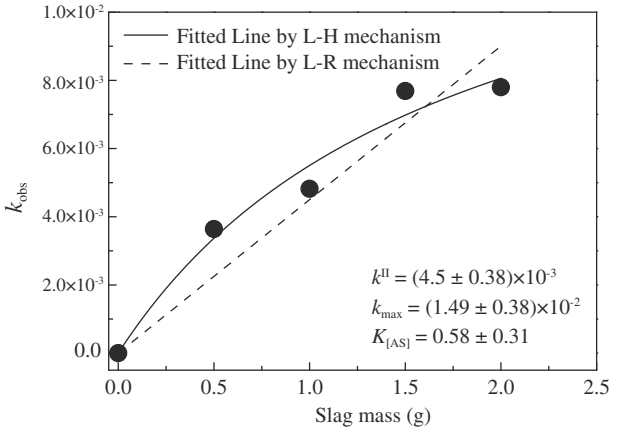

Fig. 6 – Plot of k_{obs} versus BOF-slag (0.038–0.045 mm) dosage under conditions with initial phosphorus concentration of 100 mg/L, initial pH of 7.0, and temperature of 298 K.

Generally, the smaller the size of BOF-slag, the greater the specific surface available for phosphorus adsorption. As summarized in Table S2, the specific surface area of BOF-slag exhibited a significant increase with the decrease of BOF-slag size. The specific surface area of BOF-slag with the size of 0.0–0.038 mm was larger by a factor of 2.63 than that of BOF-slag with the size of 0.10–0.180 mm. In particular, k_{obs} had a positive linear correlation with the specific surface area of BOF-slag (Fig. S3). Before being crushed and ground, metal oxides/hydroxides and silicon oxides are embedded in large BOF-slag particles. More metal oxides/hydroxides and silicon oxides are exposed with decreasing BOF-slag size during the grinding process. This can provide more active sites for phosphorus adsorption and result in the increase of k_{obs} with decreasing BOF-slag size.

It has been observed that the zeta potential of BTM (BOF-slag treated by milling) and BTA (BOF-slag treated by acid) showed a variation of surface charge from +85.8 to −40.7 and +80.2 to −35.6, respectively, when pH increased from 2.0 to 13.0 (Xue et al., 2009). This suggests that the BOF-slag surface can carry more negative charges at higher pH, which would significantly promote the repulsion of the negatively charged species in solution (Xue et al., 2009). Therefore, the decrease of k_{obs} with increasing initial pH was ascribed to the greater repulsion between phosphate groups and negatively charged surface sites.

Due to the existence of adsorbent particle–particle interactions, the decrease of the removed phosphorus per unit mass with the increase of BOF-slag dosage can be ascribed to the sorbent concentration effects in solid–water interface adsorption. In other words, the experimentally measured partition coefficient of a given system may decrease with increasing sorbent concentration, which has been observed in a number of adsorption systems and attempted to be explained by a series of models (Volce and Weber, 1985; Zhao and Hou, 2012; Zhao et al., 2013). Thus, k_{obs} may be nonlinearly dependent on BOF-slag dosage when BOF-slag dosage is high enough to enhance the sorbent concentration effects. Finally, it should be pointed out that more investigations are necessary to better understand the effects of various parameters such as temperature and pH on the kinetics and mechanisms of phosphorus removal by BOF-slag.

4. Conclusions

The batch experimental data obtained could be well fitted using the pseudo-first-order reaction model, demonstrating that the removal process of phosphorus by BOF-slag followed pseudo-first-order reaction kinetics. The apparent rate constant (k_{obs}) significantly decreased with increasing initial

phosphorus concentration, BOF-slag size, and initial pH, whereas it exhibited an opposite trend with increasing temperature and BOF-slag dosage. k_{obs} was 5.79×10^{-2} min^{-1} at initial phosphorus concentration of 50 mg/L while it was only 0.39×10^{-2} min^{-1} at initial phosphorus concentration of 125 mg/L. k_{obs} decreased by 28.0% and 42.2% with increasing BOF-slag size from 0.00–0.038 to 0.106–0.180 mm and initial pH from 3.0 to 7.0, respectively. k_{obs} increased by 47.6% and 53.3% with increasing temperature from 293 to 313 K and BOF-slag dosage from 0.5 to 2.0 g, respectively. The quantitative relationship between k_{obs} and TRP can be simply established through $k_{obs} = (3.51 \pm 0.11) \times 10^{-4} \times TRP$. Finally, it was suggested that either the Langmuir–Rideal (L–R) or Langmuir–Hinshelwood (L–H) mechanism may be appropriate for describing the removal process of phosphorus by BOF-slag.

Acknowledgments

This research was financially supported by the Fundamental Research Fund for the Central Universities (No. N130302004) and the National Natural Science Foundation of China (No. U1360204).

Appendix A. Supplementary data

Supplementary data to this article can be found online at http://dx.doi.org/10.1016/j.jes.2014.11.003.

REFERENCES

Barca, C., Gérente, C., Meyer, D., Chazarenc, F., Rès, Y., 2012. Phosphate removal from synthetic and real wastewater using steel slags produced in Europe. Water Res. 46 (7), 2376–2384.

Barca, C., Troesch, S., Meyer, D., Drissen, P., Andrès, Y., Chazarenc, F., 2013. Steel slag filters to upgrade phosphorus removal in constructed wetlands: two years of field experiments. Environ. Sci. Technol. 47 (1), 549–556.

Bowden, L.I., Jarvis, A.P., Younger, P.L., Johnson, K.L., 2009. Phosphorus removal from waste waters using basic oxygen steel slag. Environ. Sci. Technol. 43 (7), 2476–2481.

Cha, W., Kim, J., Choi, H., 2006. Evaluation of steel slag for organic and inorganic removals in soil aquifer treatment. Water Res. 40 (5), 1034–1042.

Cheung, K.C., Venkitachalam, T.H., 2000. Improving phosphate removal of sand infiltration system using alkaline fly ash. Chemosphere 41, 243–249.

Claveau-Mallet, D., Wallace, S., Comeau, Y., 2012. Model of phosphorus precipitation and crystal formation in electric arc furnace steel slag filters. Environ. Sci. Technol. 46 (3), 1465–1470.

Claveau-Mallet, D., Wallace, S., Comeau, Y., 2013. Removal of phosphorus, fluoride and metals from a gypsum mining leachate using steel slag filters. Water Res. 47 (4), 1512–1520.

Drizo, A., Forget, C., Chapuis, R.P., Comeau, Y., 2006. Phosphorus removal by electric arc furnace steel slag and serpentinite. Water Res. 40 (8), 1547–1554.

Gong, G.Z., Ye, S.F., Tian, Y.J., Wang, Q., Ni, J.D., Chen, Y.F., 2009. Preparation of a new sorbent with hydrated lime and blast furnace slag for phosphorus removal from aqueous solution. J. Hazard. Mater. 166 (2–3), 714–719.

House, W.A., 1999. The physico-chemical conditions for the precipitation of phosphate with calcium. Environ. Technol. 20 (7), 727–733.

Jha, V.K., Kameshima, Y., Nakajima, A., Okada, K., 2004. Hazardous ions uptake behavior of thermally activated steel-making slag. J. Hazard. Mater. 114 (1–3), 139–144.

Jha, V.K., Kameshima, Y., Nakajima, A., Okada, K., 2008. Utilization of steel-making slag for the uptake of ammonium and phosphate ions from aqueous solution. J. Hazard. Mater. 156 (1–3), 156–162.

Johansson-Westholm, L., 2006. Substrates for phosphorus removal-potential benefits for on-site wastewater treatment? Water Res. 40 (1), 23–36.

Karaca, S., Gürses, A., Ejer, M., Açıkyıldız, M., 2006. Adsorption removal of phosphate from aqueous solutions using raw and calcinated dolomite. J. Hazard. Mater. 128 (2–3), 273–279.

Khelifi, O., Kozuki, Y., Murakami, H., Kurata, K., Nishioka, M., 2002. Nutrients adsorption from seawater by new porous carrier made from zeolitized fly ash and slag. Mar. Pollut. Bull. 45 (1–12), 311–315.

Kostura, B., Kulveitová, H., Leško, J., 2005. Blast furnace slags as sorbents of phosphate from water solutions. Water Res. 39 (9), 1795–1802.

Lee, M.S., Drizo, A., Rizzo, D.M., Druschel, G., Hayden, N., Twohig, E., 2010. Evaluating the efficiency and temporal variation of pilot-scale constructed wetlands and steel slag phosphorus removing filters for treating dairy wastewater. Water Res. 44 (14), 4077–4086.

Li, Y.Z., Liu, C.J., Luan, Z.K., Peng, X.J., Zhu, C.L., Chen, Z.Y., et al., 2006. Phosphate removal from aqueous solutions using raw and activated red mud and fly ash. J. Hazard. Mater. 137 (1), 374–383.

Li, H.B., Li, Y.H., Gong, Z.Q., Li, X.D., 2013. Performance study of vertical flow constructed wetlands for phosphorus removal with water quenched slag as a substrate. Ecol. Eng. 53, 39–45.

Oguz, E., 2005. Thermodynamic and kinetic investigations of PO43– adsorption on blast furnace slag. J. Colloid Interface Sci. 281 (1), 62–67.

Pratt, C., Shilton, A., Pratt, S., Haverkamp, R.G., Bolan, N.S., 2007a. Phosphorus removal mechanisms in active slag filters treating waste stabilization pond effluent. Environ. Sci. Technol. 41 (9), 3296–3301.

Pratt, C., Shilton, A., Pratt, S., Haverkamp, R.G., Elmetri, I., 2007b. Effects of redox potential, and pH changes on phosphorus retention by melter slag filters treating wastewater. Environ. Sci. Technol. 41 (18), 6585–6590.

Shilton, A.N., Elmetri, I., Drizo, A., Pratt, S., Haverkamp, R.G., Bilby, S.C., 2006. Phosphorus removal by an 'active' slag filter—a decade of full scale experience. Water Res. 40 (1), 113–118.

Søvik, A.K., Kløve, B., 2005. Phosphorus retention processes in shell sand filter systems treating municipal wastewater. Ecol. Eng. 25 (2), 168–182.

Valsami-Jones, E., 2001. Mineralogical controls on phosphorus recovery from wastewaters. Mineral. Mag. 65 (5), 611–620.

Vohla, C., Kõiv, M., Bavor, H.J., Chazarenc, F., Mander, U., 2011. Filter materials for phosphorus removal from wastewater in treatment wetlands—a review. Ecol. Eng. 37 (1), 70–89.

Volce, T.C., Weber, W.J., 1985. Sorbent concentration effects in liquid/solid partitioning. Environ. Sci. Technol. 19 (9), 789–796.

Wang, S., Yang, J., Lou, S.J., Yang, J., 2010. Wastewater treatment performance of a vermifilter enhancement by a converter slag–coal cinder filter. Ecol. Eng. 36 (4), 489–494.

Xiong, J.B., He, Z.L., Mahmood, Q., Liu, D., Yang, X.E., Islam, E., 2008. Phosphate removal from solution using steel slag through magnetic separation. J. Hazard. Mater. 152 (1), 211–215.

Xue, Y.J., Hou, H.B., Zhu, S.J., 2009. Characteristics and mechanisms of phosphate adsorption onto basic oxygen furnace slag. J. Hazard. Mater. 162 (2–3), 973–980.

Yang, Y., Tomlinson, D., Kennedy, S., Zhao, Y.Q., 2006. Dewartered alum sludge: a potential adsorbent for phosphorus removal. Water Sci. Technol. 54 (5), 207–213.
Yang, J., Wang, S., Lu, Z.B., Yang, J., Lou, S.J., 2009. Converter slag–coal cinder columns for the removal of phosphorous and other pollutants. J. Hazard. Mater. 168 (1), 331–337.
Zeng, L., Li, X.M., Liu, J.D., 2004. Adsorptive removal of phosphate from aqueous solutions using iron oxide tailings. Water Res. 38 (5), 1318–1326.
Zhao, L.X., Hou, W.G., 2012. The effect of sorbent concentration on the partition coefficient of pollutants between aqueous and particulate phases. Colloids Surf. A Physicochem. Eng. Asp. 396, 29–34.
Zhao, L.X., Song, S.E., Du, N., Hou, W.G., 2013. A sorbent concentration-dependent Freundlich isotherm. Colloid Polym. Sci. 291 (3), 541–550.

Editorial Board of Journal of Environmental Sciences

JOURNAL OF ENVIRONMENTAL SCIENCES

环境科学学报(英文版)

www.jesc.ac.cn

Aims and scope

Journal of Environmental Sciences is an international academic journal supervised by Research Center for Eco-Environmental Sciences, Chinese Academy of Sciences. The journal publishes original, peer-reviewed innovative research and valuable findings in environmental sciences. The types of articles published are research article, critical review, rapid communications, and special issues.

The scope of the journal embraces the treatment processes for natural groundwater, municipal, agricultural and industrial water and wastewaters; physical and chemical methods for limitation of pollutants emission into the atmospheric environment; chemical and biological and phytoremediation of contaminated soil; fate and transport of pollutants in environments; toxicological effects of terrorist chemical release on the natural environment and human health; development of environmental catalysts and materials.

For subscription to electronic edition

Elsevier is responsible for subscription of the journal. Please subscribe to the journal via http://www.elsevier.com/locate/jes.

For subscription to print edition

China: Please contact the customer service, Science Press, 16 Donghuangchenggen North Street, Beijing 100717, China. Tel: +86-10-64017032; E-mail: journal@mail.sciencep.com, or the local post office throughout China (domestic postcode: 2-580).

Outside China: Please order the journal from the Elsevier Customer Service Department at the Regional Sales Office nearest you.

Submission declaration

Submission of the work described has not been published previously (except in the form of an abstract or as part of a published lecture or academic thesis), that it is not under consideration for publication elsewhere. The publication should be approved by all authors and tacitly or explicitly by the responsible authorities where the work was carried out. If the manuscript accepted, it will not be published elsewhere in the same form, in English or in any other language, including electronically without the written consent of the copyright-holder.

Editorial

Authors should submit manuscript online at http://www.jesc.ac.cn. In case of queries, please contact editorial office, Tel: +86-10-62920553, E-mail: jesc@rcees.ac.cn. Instruction to authors is available at http://www.jesc.ac.cn.

Journal of Environmental Sciences (Established in 1989)
Volume 30 2015

Supervised by	Chinese Academy of Sciences	**Published by**	Science Press, Beijing, China
Sponsored by	Research Center for Eco-Environmental		Elsevier Limited, The Netherlands
	Sciences, Chinese Academy of Sciences	**Distributed by**	
Edited by	Editorial Office of Journal of	Domestic	Science Press, 16 Donghuangchenggen
	Environmental Sciences		North Street, Beijing 100717, China
	P. O. Box 2871, Beijing 100085, China		Local Post Offices through China
	Tel: 86-10-62920553; http://www.jesc.ac.cn	Foreign	Elsevier Limited
	E-mail: jesc@rcees.ac.cn		http://www.elsevier.com/locate/jes
Editor-in-chief	X. Chris Le	**Printed by**	Beijing Beilin Printing House, 100083, China

CN 11-2629/X **Domestic postcode: 2-580** **Domestic price per issue RMB ¥ 110.00**

ISSN 1001-0742